Quantum effects in percolation systems. Granular $Cu_{1-x}O_x$ films

A. G. Aronov, M. E. Gershenzon, and Yu. E. Zhuravlev

Institute of Radio Engineering and Electronics, Academy of Sciences of the USSR; B. P. Konstantinov Leningrad Institute of Nuclear Physics, Academy of Sciences of the USSR, Gatchina

(Submitted 5 April 1984)
Zh. Eksp. Teor. Fiz. **87**, 971–988 (September 1984)

An experimental and theoretical study is made of the manifestations of quantum effects in macroscopically inhomogeneous systems for the particular case of granular metals. Far from the metal-insulator transition, which in the investigated granular $Cu_{1-x}O_x$ films is due to percolation effects, the behavior of the conductivity of these films is adequately described by the theory developed for homogeneous conductors. As the metal-insulator transition is approached, the macroscopic inhomogeneity of the samples manifests itself in the appearance of quantum effects. Allowance for the macroscopic inhomogeneity permits a quantitative description of the observed suppression of the localized contribution by the magnetic field. However, the proposed theory fails to explain the temperature dependence of the conductivity.

1. INTRODUCTION

In recent years there has been considerable interest in the metal-insulator transition observed upon increasing disorder in systems having a metallic conductivity.[1] In principle, an increase in the disorder can enhance both macroscopic potential fluctuations having a characteristic scale of the order of the wavelength of an electron with the Fermi energy and also fluctuations having a considerably larger scale. When only large-scale fluctuations are present in the conductor the metal-insulator transition is classical in nature and is due to the formation of a percolating structure as the result of a division of the conductor into classically allowed and forbidden regions for conduction electrons.[2] Examples of macroscopically inhomogeneous systems are the cermets—metallic grains embedded in an insulating matrix. In the case of microscopic potential fluctuations (macroscopically homogeneous systems) the transition from a metallic conductivity to an activational conductivity is due to quantum effects, both single-particle (Anderson localization of electrons)[3] and many-particle (strengthening of the electron-electron interaction with increasing disorder)[4] effects. In the general case, when potential fluctuations of various length scales are present, the phase transition is governed by a superposition of quantum and classical effects.[5,6]

At $T=0$ the proximity to the transition point is characterized by a correlation length ξ which tends to infinity as the transition is approached from either the metal or insulator side. Spin-flip or inelastic electron scattering processes at $T\neq 0$ lead to a phase disturbance [with frequency $(\tau_\varphi)^{-1}$] of the electron wave function and give rise to an additional length scale in the region of metallic conductivity—the diffusion length $L=(D\tau_\varphi)^{1/2}$ over the time of the phase disturbance τ_φ (D is the electron diffusion coefficient). The analogous role for the electron-electron interaction effects is played by the coherence length $L_T=(\hbar D/kT)^{1/2}$ in the normal metal, i.e., the length over which the wave functions of two quasiparticles with energy difference $\sim kT$ maintain their spatial coherence. The main features of the metal-insulator transition depend importantly on the dimensions of the disordered system in relation to these length scales.

Experimentally, the metal-insulator transition which occurs upon increasing disorder in three-dimensional conductors has been studied in heavily doped semiconductors[7–11] and in rather thick disordered metal films.[12–17] The semiconductor samples studied in Refs. 7–11, particularly the neutron-doped samples, have a high degree of homogeneity and are amenable to treatment by the quantum scaling theory of the metal-insulator transition.[3,18,19] On the other hand, it appears that the disordered metals studied in Refs. 12–17 characteristically contain (to some degree or other) macroscopic inhomogeneities, and this circumstance is not always taken into account in discussing the experimental results near the metal-insulator transition. The present study was therefore undertaken to investigate experimentally the metal-insulator transition in conductors having macroscopic fluctuations of the potential (for the particular case of granular metal films) and to examine the manifestations of quantum effects in conductors of this type. In addition, the phenomena of weak localization and electron-electron interaction, previously studied mainly in semiconductors[20–23] and semimetals,[24] were studied in detail in slightly disordered three-dimensional metal films.

The rather thick disordered copper-oxygen films investigated in the present study have a granular structure. The development of this structure with increasing oxygen concentration in the films leads to a transition from a metallic conductivity to an activational conductivity. The experimental data indicate that this metal-insulator transition is of a classical (percolational) character. For slightly disordered samples ($\xi<L_\varphi, L_T$) the dependence of the conductivity σ on the temperature T and magnetic field H is adequately described by the existing theory of weak localization and electron-electron interaction in macroscopically homogeneous disorderd metals. The macroscopic inhomogeneity of the samples begins to manifest itself as the system approaches the metal-insulator transition, at which the condition $\xi<L_\varphi L_T$ breaks down. For this case we obtain theoretically the functional dependences $\sigma(T)$ and $\sigma(H)$ due to localization effects with allowance for the spatial dispersion of the electron diffusion coefficient D at distances smaller than ξ. Comparison of the experimental data with the theory has

 0038-5646/84/090554-10$04.00

yielded not only a series of relaxation times for the conduction electrons but also an estimate of ξ for samples with metallic conductivity. The temperature dependence obtained for the relaxation time of the phase of the electron wave function indicates that with increasing disorder the electron-electron interaction comes to govern the electron energy relaxation. On the insulator side of the transition and at sufficiently low temperatures ($T < T_0$), the conductivity is of an activational character [$\rho = \rho_0 \exp(T_0/T)^{1/2}$] and a negative magnetoresistance is observed, the relative size of which, $\log[\rho(T,H)/\rho(T,O)]$, is proportional to $\log[\rho(T)/\rho_0]$.

This article is structured as follows: In Sec. 2 we present the previously obtained theoretical results which we shall need and the results of a treatment of quantum effects in metals in the presence of macroscopic potential fluctuations. In Sec. 3 we briefly discuss the sample-preparation and experimental techniques. In Sec. 4 we describe the experimental results and compare them with the theory.

2. THEORY

We restrict our further discussion to the case in which the large-scale fluctuations are dominant, i.e., there is a random metal network near the metal-insulator transition (as we shall see, it was precisely this situation that was realized in the experiment, the percolation path being formed by random bridges between granules).

According to the theory of percolation near a metal-insulator transition at $T = 0$, the correlation length and the conductivity depend on the proximity to the transition point according to the power law[2]

$$\xi \sim |1-n/n_c|^{-\nu}, \quad \sigma_0 \sim (1-n/n_c)^t \sim \xi^{-\tilde{t}}, \quad \tilde{t}=t/\nu, \tag{1}$$

where in the three-dimensional case ($d = 3$) one has $t \approx 1.7$–1.9, $\nu \approx 0.8$–0.9, so that $\tilde{t} = 2$, while for $d = 2$ one has $t \approx \nu \approx 1.3$ and $\tilde{t} \approx 1$. The quantity n characterizes the concentration of the insulator, with n_c being the critical concentration at which the metal-insulator transition occurs.

At values of n corresponding to the condition $L_\varphi, L_T \gg \xi$ there is no spatial dispersion of the diffusion coefficient at distances of the order of L_φ, L_T, and the macroscopic inhomogeneity should not manifest itself in the appearance of quantum effects. For macroscopically inhomogeneous conductors ($L_\varphi L_T \gg \xi$) the localization and interaction effects are manifested as small quantum corrections to the conductivity, with an anomalous dependence on the temperature and magnetic field. The magnetoresistance $mc/e\tau$ of disordered normal metals for fields in the region $H \ll kT/g_L\mu$ (g_L is the Landé factor, μ is the Bohr magneton, and τ is the relaxation time of the electron momentum) is mainly due to localization effects, since in these metals the interaction of electrons having a small combined momentum is weak.[25] For three-dimensional samples whose thickness a is much larger than L_φ the magnetoresistance should be isotropic with respect to the relative orientation of the film plane and the field. We note that because $L_\varphi(T,H) \sim \min\{L_\varphi(T), L_H\}$ in a magnetic field [here $L_H = (\hbar c/2eH)^{1/2}$ is the magnetic length], in sufficiently strong fields ($L_H \ll a$) films with $a \lesssim L_\varphi(T)$ are also three-dimensional. The function $\sigma(H)$ obtained in the weak-localization theory for the three-dimensional case under the condition $E_F\tau \gg 1$ is of the form

$$\sigma(O)-\sigma(H) \equiv \Delta\sigma(H) = -\frac{e^2}{2\pi^2\hbar}\left(\frac{eH}{\hbar c}\right)^{1/2} \times\left\{\frac{3}{2} f\left(2\frac{L_\varphi^{*2}}{L_H^2}\right) - \frac{1}{2} f\left(2\frac{L_\varphi^2}{L_H^2}\right)\right\}, \tag{2}$$

where

$$L_\varphi^* = (D\tau_\varphi^*)^{1/2}, \quad f(x) = \begin{cases} \frac{1}{48}x^{3/2}, & x \ll 1 \\ 0.605, & x \gg 1 \end{cases}$$

Expression (2) is written with allowance for the spin-orbit interaction. The phase relaxation time τ_φ of the electron wave function and the modified (incorporating the spin-orbit interaction) time τ_φ^* are given by the expressions[27]:

$$\tau_\varphi^{-1} = \tau_\varepsilon^{-1} + 2\tau_s^{-1}, \quad \tau_\varphi^{*-1} = \tau_\varepsilon^{-1} + {}^2/_3\tau_s^{-1} + {}^4/_3\tau_{so}^{-1}, \tag{3}$$

where τ_ε is the electron energy relaxation time, τ_s is the characteristic time for spin-flip elastic scattering of electrons on magnetic impurities, and τ_{so} is the spin relaxation time for the spin-orbit interaction.

The temperature dependence of the quantum corrections to the conductivity of normal metals should be governed by both localization and the interaction between electrons having nearly equal energies and momenta (the so-called diffusion channel of interaction). For three-dimensional samples the function $\sigma(T)$ at $H = 0$ is of the form[3,4,18]

$$\sigma(T_1)-\sigma(T_2) = \frac{e^2}{2\pi^2\hbar}\left\{\frac{3}{2}\left[\frac{1}{L_\varphi^*(T_1)} - \frac{1}{L_\varphi^*(T_2)}\right] - \frac{1}{2}\left[\frac{1}{L_\varphi(T_1)} - \frac{1}{L_\varphi(T_2)}\right] + 0.915\left[\frac{2}{3} - \varphi(F)\right]\left[\frac{1}{L_T(T_1)} - \frac{1}{L_T(T_2)}\right]\right\}, \tag{4}$$

where the first two terms in the braces describe the localization contribution with allowance for the spin-orbit interaction, the third term is the contribution of the diffusion channel, and the function φ goes to zero as $F \to 0$ (F is the screening parameter). We note that in the three-dimensional case the contribution to $\sigma(T)$ due to the interaction effects should outweigh that due to the localization effects by virtue of the condition $\tau_\varphi \gg \hbar/kT$, which must be satisfied in order for (2) and (4) to apply. In sufficiently strong fields ($H \gg \hbar c/4eD\tau_\varphi^*$) the temperature dependence of the localization contribution should be suppressed, while the temperature dependence $\sigma(T)$ due to the interaction in the diffusion channel remains unchanged for $H \lesssim kT/g_L\mu$.

As the system approaches the metal-insulator transition, the correlation length ξ grows, and at some values of n and T the condition $\xi < L_\varphi, L_T$ breaks down. In this case the spatial dispersion of the electron diffusion coefficient becomes important at the characteristic length scales for the localization and interaction effects. The length $\mathscr{L}_\varphi$ over which the phase coherence of the electron wave function is maintained can in this case be determined from the following considerations. By definition, $\mathscr{L}_\varphi$ is given by

$$\mathscr{L}_\varphi = (D(\mathscr{L}_\varphi)\tau_\varphi)^{1/2}, \tag{5}$$

where $D(\mathscr{L}_\varphi)$ is the diffusion coefficient on the scale of $\mathscr{L}_\varphi$.

$$D(\mathscr{L}) = \frac{\sigma(\mathscr{L})}{\frac{\partial n}{\partial \mu}(\mathscr{L})} = D \begin{cases} 1, & \mathscr{L} \gg \xi, \\ (\xi/\mathscr{L})^{\tilde{t}-\tilde{\beta}}, & \mathscr{L} \ll \xi. \end{cases} \tag{6}$$

Here we have taken into account that the conductivity involves only those electrons belonging to an infinite cluster,[6] the power $P(\mathscr{L})$ of which is[2]

$$P(\mathscr{L}) = P \begin{cases} 1, & \mathscr{L} \gg \xi, \\ (\xi/\mathscr{L})^{\tilde{\beta}}, & \mathscr{L} \ll \xi, \end{cases} \tag{7}$$

$$P \approx (1-n/n_c)^{\beta} \sim \xi^{-\tilde{\beta}}, \quad \tilde{\beta} = \beta/\nu.$$

The quantity D in (6) is the macroscopic diffusion coefficient, which is proportional to $(1-n/n_c)^{t-\beta}$. Expression (6) is valid for values of $\mathscr{L}$ which are much larger than the granule dimension b. When $\mathscr{L}_\varphi$ and $\mathscr{L}_T$ are smaller than b, the quantum corrections $\Delta\sigma_{\text{mic}}(T,H)$ to the conductivity on the scale of $\mathscr{L}_\varphi$ and $\mathscr{L}_T$ are converted into the measurable quantity $\Delta\sigma(T,H)$ in accordance with the scaling hypothesis $\Delta\sigma(T,H) = \Delta\sigma_{\text{mic}}(T,H)(1-n/n_c)^t$. For $b \ll \mathscr{L}_\varphi \ll \xi$, we find,[6] using (5) and (6),

$$\mathscr{L}_\varphi = (D\tau_\varphi \xi^{\tilde{t}-\tilde{\beta}})^{(2+\tilde{t}-\tilde{\beta})^{-1}} \equiv (L_\varphi{}^2 \xi^{\tilde{t}-\tilde{\beta}})^{(2+\tilde{t}-\tilde{\beta})^{-1}}. \tag{8a}$$

The coherence length $\mathscr{L}_T$ of the normal metal can be determined in an analogous way as

$$\mathscr{L}_T = \left(\frac{\hbar D}{kT}\xi^{\tilde{t}-\tilde{\beta}}\right)^{(2+\tilde{t}-\tilde{\beta})^{-1}} \equiv (L_T{}^2 \xi^{\tilde{t}-\tilde{\beta}})^{(2+\tilde{t}-\tilde{\beta})^{-1}}. \tag{8b}$$

We stress that neither $\mathscr{L}_\varphi$ nor $\mathscr{L}_T$ depends on ξ, i.e., on the proximity to the metal-insulator transition, since $D \sim \xi^{\beta-t}$.

To obtain the localization corrections to the conductivity it is necessary to take into account not only the spatial dispersion of the diffusion coefficient but also the change in the normalization of the diffusion (Cooper) pole. Therefore,

$$\frac{\Delta\sigma}{\sigma} = -\frac{2}{\pi\nu}\int \frac{dq}{P(q)\,[D(q)q^2 + 1/\tau_\varphi]}, \tag{9}$$

where ν is the density of states in the metal. Using Eqs. (6), (7), and (9), we find that the correction to the conductivity with allowance for the spin-orbit interaction is of the form

$$\Delta\sigma(T) = -\frac{e^2}{\pi^2}\frac{1}{\tilde{t}-\tilde{\beta}+2}\operatorname{cosec}\left[\frac{\pi(3-\tilde{\beta})}{\tilde{t}-\tilde{\beta}+2}\right] \times\left\{\frac{3}{2}\frac{1}{\mathscr{L}_\varphi{}^*}\left(\frac{\mathscr{L}_\varphi{}^*}{\xi}\right)^{\tilde{t}} - \frac{1}{2\mathscr{L}_\varphi}\left(\frac{\mathscr{L}_\varphi}{\xi}\right)^{\tilde{t}}\right\}. \tag{10}$$

We note that expression (10) corresponds to the scaling theory for percolational metal-insulator transitions. In fact, since

$$\Delta\sigma(\xi)/\sigma(\xi) = \Delta\sigma(\mathscr{L})/\sigma(\mathscr{L}), \tag{11}$$

the observed correction $\Delta\sigma(\xi)$ should be of the form

$$\Delta\sigma(\xi) = \Delta\sigma(\mathscr{L})\frac{\sigma(\xi)}{\sigma(\mathscr{L})} = \Delta\sigma(\mathscr{L})\left(\frac{\mathscr{L}}{\xi}\right)^{\tilde{t}}, \tag{12}$$

which agrees with expression (10).

The presence of a magnetic field gives rise to a new length scale L_H. Therefore

$$\Delta\sigma(H) = -\frac{e^2}{2\pi^2\hbar}\frac{1}{\mathscr{L}_\varphi}\left(\frac{\mathscr{L}_\varphi}{\xi}\right)^{\tilde{t}}\overline{\Phi}\left(\frac{L_H{}^2}{\mathscr{L}_\varphi{}^2}\right). \tag{13}$$

For $\mathscr{L}_\varphi \gg \mathscr{L}_H$, $\Delta\sigma(H)$ ceases to depend on $\mathscr{L}_\varphi$:

$$\Delta\sigma(H) \sim \frac{e^2}{2\pi^2\hbar}\frac{1}{L_H}\left(\frac{L_H}{\xi}\right)^{\tilde{t}} \sim H^{(1-\tilde{t})/2}. \tag{14}$$

Since $\tilde{t} > 1$ in the three-dimensional case, according to (14) the quantum correction to the conductivity goes to zero with increasing magnetic field, while the magnetoresistance goes to saturation. In the small-field region we have $\overline{\Phi} \sim \text{const} + H^2$. Unfortunately, the function $\overline{\Phi}(x)$ cannot be calculated explicitly for arbitrary $\tilde{t}$ and $\tilde{\beta}$. Therefore, we did the calculation under the assumption that $\tilde{t} = 2$ and $\tilde{\beta} = 0$. The relation $\tilde{t} = 2$ is satisfied to good accuracy in the three-dimensional case.[2] As to the second condition, Shklovskiĭ and Éfros[2] give $\tilde{\beta} \approx 0.5 \ll \tilde{t}$, and, furthermore, according to (14) the asymptotic expression for $\Delta\sigma(H)$ is not governed at all by the exponent $\tilde{\beta}$, which can enter only in the numerical coefficients. Under these assumptions and with allowance for the spin-orbit interaction we have

$$\Delta\sigma(H) - \Delta\sigma(0) = -\frac{e^2}{2\pi^2\hbar}\left\{\frac{3}{2}\frac{1}{\mathscr{L}_\varphi{}^*}\left(\frac{\mathscr{L}_\varphi{}^*}{\xi}\right)^2 \times\Phi\left(\frac{L_H{}^2}{\mathscr{L}_\varphi{}^2}\right) - \frac{1}{2}\frac{1}{\mathscr{L}_\varphi}\left(\frac{\mathscr{L}_\varphi}{\xi}\right)^2\Phi\left(\frac{L_H{}^2}{\mathscr{L}_\varphi{}^2}\right)\right\}, \tag{15}$$

where

$$\Phi(x) = \frac{1}{2(\pi x)^{1/2}}\int_0^\infty \frac{dz}{z^{1/2}}\frac{\sin xz}{\operatorname{sh} z} - \frac{1}{\sqrt{2}}.$$

The dependence of the magnetoresistance on the magnetic field is shown in Fig. 1 for various values of the ratio $\tau_\varphi/\tau_\varphi^*$. One notices that the position of the maximum is independent of $\tau_\varphi/\tau_\varphi^*$ for $\tau_\varphi \gg \tau_\varphi^*$. This circumstance is due to the fact that this ratio appears in the equation for the position of the maxi-

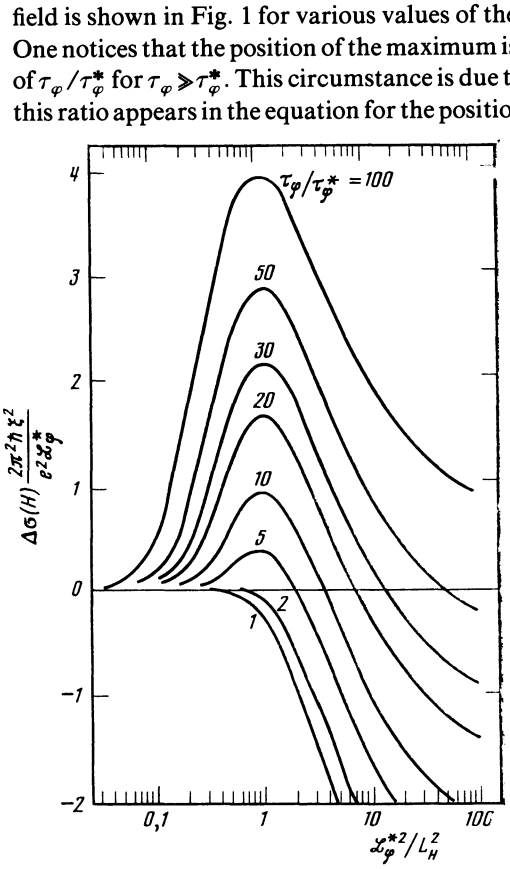

FIG. 1. Calculated dependence of $(\Delta\sigma(H)2\pi^2\hbar\xi^2)/e^2\mathscr{L}_\varphi^*$ on $(\mathscr{L}_\varphi^{*2}/L_H{}^2)$ according to (15) for various values of $\tau_\varphi/\tau_\varphi^*$.

mum in the form $(\tau_\varphi/\tau_\varphi^*)^{1/8}$, and so the position of the maximum is insensitive even to strong changes in this parameter. It follows from (15) that in large fields the magnetoresistance approaches saturation as const $- 1/H^{1/2}$, in agreement with (14) for $\tilde{t} = 2$. We stress that all the expressions (10), (14), and (15) are valid as long as the quantum corrections to the conductivity are small compared to the conductivity itself.

3. EXPERIMENTAL TECHNIQUE

The sample films were prepared by rf sputtering of 99.999% pure copper in an argon atmosphere with a small ($\lesssim 2\%$) admixture of oxygen for creating a controlled degree of disorder. The vacuum chamber was first pumped down to $2\cdot10^{-6}$ mbar at a rate of 400 liter/sec with a turbomolecular pump; at the time of the sputtering, which was done without decreasing the rate of evacuation, the total pressure of argon and oxygen was $1\cdot10^{-2}$ mbar. The copper was sputtered at a rate of 430 Å/min onto glass substrates at room temperature. An interference microscope was used to calibrate the sputtering rate and to determine the thickness of the films. The films were deposited in layers—after a layer of thickness $\gamma \gtrsim 50$ Å was deposited, the substrate was covered up for 30 sec. The cycle was then repeated. As will be seen, the layer-by-layer deposition enabled us to vary the dimension b of the crystallites (granules)—for $\gamma \lesssim 500$ Å the value of b turned out to be comparable to the layer thickness. The results presented below were obtained mainly for samples with $\gamma = 140$ Å. The resistivity of the films varied over wide limits depending on the oxygen partial pressure P_{O_2}. The $\rho(P_{O_2})$ curves measured at 300 K and 4.2 K for films with $\gamma = 140$ Å are shown in Fig. 2. Curves of similar shape for the dependence of ρ on the degree of disorder have been observed for granular films of various metals.[15,28] The uniformity of the oxygen distribution over the thickness of the films was monitored by Auger spectroscopy over the course of an ion etching. The oxygen concentration in the films was determined by ESCA; it was thereby established[1)] that all the oxygen in the interior of the films was bound into cuprous oxide, CuO_2. The dependence on P_{O_2} of the percent oxygen content in the films is shown in Fig. 2. A scanning electron microscope study of the films revealed a granular structure with an average granule dimension $b \approx (100–300)$ Å. Such a structure is often realized upon the joint evaporation of a metal and an insulator[17,28] or upon the sputtering of a metal in the presence of oxygen,[13] where it turns out that relatively pure metal inside the granules is enclosed in an insulating coating. The ESCA data suggest that in the present case the films consist of crystallites (granules) of relatively pure metal with their surfaces coated with a layer of cuprous oxide. That the films under study have such a structure is confirmed by the entire set of experimental data described below.

The resistance R of the samples was measured in a dc current with a digital ohmmeter having a relative precision of $\Delta R/R = 1\cdot10^{-6}$. To provide a high accuracy of the resistance measurements at values of the measuring current ~ 1 μA, samples of various geometries were prepared from the films by photolithography. For example, the samples with resistivities $\rho \lesssim 1\cdot10^{-4}$ Ω·cm consisted of a 20-μm wide stripe which was bent into the shape of a meander with a total length of 60 cm. For measuring the resistance of samples with $\rho \approx (1\cdot10^3–1\cdot10^5)$ Ω·cm it is important to keep the field strength E low in order to maintain ohmicity (a substantial field nonlinearity for samples of this type was observed at $T = 4$ K in fields $E \gtrsim 1$ V/cm). Therefore, for $\rho \gtrsim 1\cdot10^3$ Ω·cm we used samples in the form of films 1-cm wide, while the values of the measuring current were decreased to $1\cdot10^{-10}$ A. The temperature dependence of the resistance was measured at temperatures from 1.5 to 300 K; the magnetoresistance was determined at $T = (1.5–30)$ K in magnetic fields with strengths up to 60 kOe, produced by a superconducting solenoid. For all the films studied the magnetoresistance was to good accuracy independent of the relative orientation of the field and film plane. The isotropicity of the magnetoresistance at arbitrary values of H (a characteristic indicator that a sample is three-dimensional) was maintained by choice of sample thickness (this is why a is larger for films with smaller ρ).

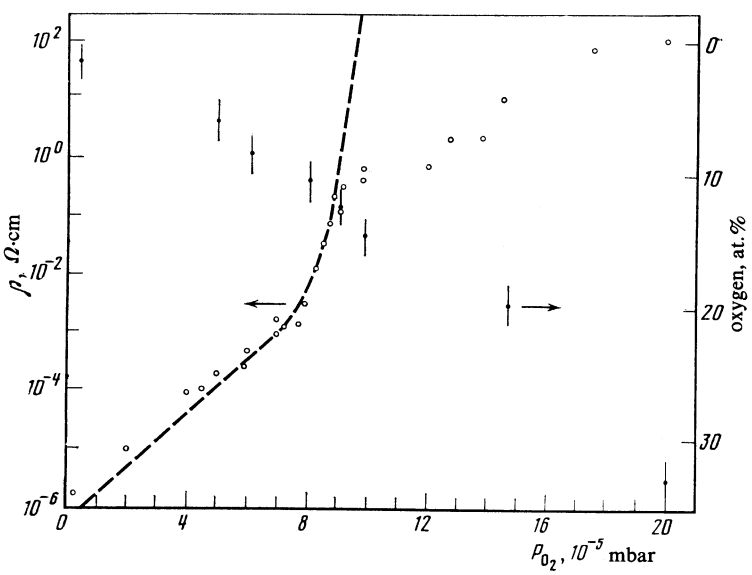

FIG. 2. Measured resistivity ρ of films with $\gamma = 140$ Å at $T = 300$ K (○) and $T = 4.2$ K (dashed curve) and the oxygen concentration in these films (●), plotted as functions of the oxygen partial pressure P_{O_2}.

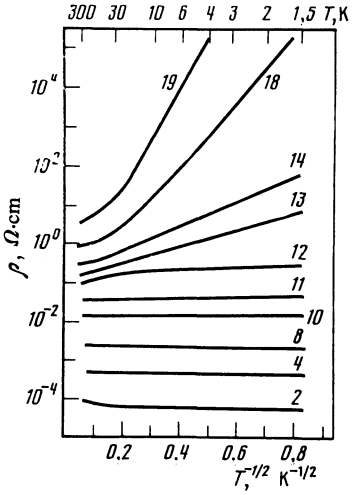

FIG. 3. Temperature dependence of the resistivity of a series of samples (the samples are numbered in accordance with Table I).

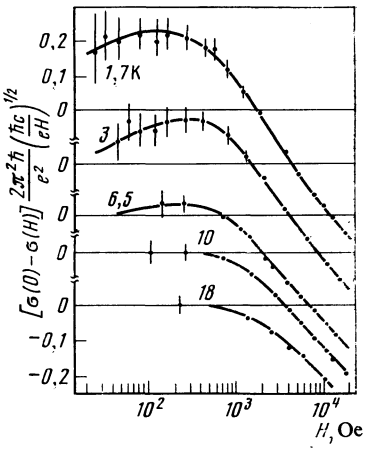

FIG. 4. Curves of $\Delta\sigma(H)$ measured at various temperatures for sample No. 2. (For samples with larger values of ρ the experimental error in determining $\Delta\sigma(H)$ is substantially smaller.) The solid lines correspond to the theoretical curves (2) calculated for the values of τ_φ and τ_φ^* given in Fig. 5.

4. EXPERIMENTAL RESULTS AND DISCUSSION

The temperature dependence of the resistivity of a series of samples is shown in Fig. 3. With increasing disorder of the films one observes a transition from a metallic conductivity to an activational conductivity. An analogous shape of the temperature curves of ρ in the vicinity of the metal-insulator transition with increasing disorder has been observed previously in heavily doped semiconductors and granular metals (see, e.g., Refs. 9 and 13–17). In analyzing the experimental data, one can agree to distinguish between three resistivity intervals in which the $\rho(T)$ curves of the films behave in a similar way [as we shall see, the same goes for the $\rho(H)$ curves]. Films with $\rho \lesssim 1\cdot10^{-3}$ Ω cm (samples No. 1–7 in Table I) exhibit a decrease in the resistance as the temperature is lowered from 300 to 30 K, followed by a growth described by a function $\rho(T)$ which is similar in shape to a square-root curve. In the interval $\rho \approx (1\cdot10^{-3}$–$0.5)$ Ω·cm [samples No. 8–12 and also the high-temperature parts of the $\rho(T)$ curves for samples No. 13–17] the growth of the resistance with decreasing temperature is also described by a power law, but with a different exponent. The temperature interval in which the values of ρ decrease with decreasing T on account of the "freezing out" of the phonons gradually narrows and disappears entirely at $\rho \approx 1\cdot10^{-2}$ Ω·cm. Finally, at $\rho \gtrsim 0.5$ Ω·cm (the low-temperature parts of the $\rho(T)$ curves for samples No. 13–19) the conductivity is activational in character, described by a function $\rho(T) \sim \exp(T_0/T)^{1/2}$. In what follows we shall give a more detailed analysis of typical $\rho(T)$ and $\rho(H)$ curves for the different intervals of change in ρ.

4.1. $\rho < 1\cdot10^{-3}$ Ω·cm

Figure 4 shows typical $\sigma(H)$ curves obtained at various temperatures for films with $\rho < 1\cdot10^{-3}$ Ω·cm (sample No. 2). For $T \gtrsim 10$ K the magnetoresistance is negative, while for $T \lesssim 10$ K we observe a transition from a positive to a negative magnetoresistance with increasing H. The theoretical curves (2) are shown by solid lines in Fig. 4; the values of $D\tau_\varphi(T)$ and $D\tau_\varphi^*(T)$ were used as adjustable parameters in comparing the theory and experiment. The qualitative behavior of the $\sigma(H)$ curves, which is determined by the relationship between τ_φ and τ_φ^*, changes with temperature in the same way as for two-dimensional films of normal metals.[29–31]

TABLE I.

Sample No.	ρ (300 K), Ω·cm	a, 10^3 Å	P_{O_2}, 10^{-5} mbar	τ_{so}, 10^{-11} sec	T_0, K	σ_0, S/cm
1	$5{,}6\cdot10^{-5}$	12	3,5	3,1	–	$2{,}0\cdot10^4$
2	$6{,}6\cdot10^{-5}$	10	3,5	3,1	–	$1{,}7\cdot10^4$
3	$1{,}6\cdot10^{-4}$	10	4,8	4,5	–	$7{,}7\cdot10^3$
4	$4{,}4\cdot10^{-4}$	2,5	6,1	2,7	–	$2{,}4\cdot10^3$
5	$4{,}9\cdot10^{-4}$	3,6	6,3	2,8	–	$2{,}1\cdot10^3$
6	$9{,}8\cdot10^{-4}$	5,8	7,1	–	–	1090
7	$9{,}6\cdot10^{-4}$	3,6	7,1	–	–	810
8	$2{,}5\cdot10^{-3}$	2,5	7,8	–	–	390
9	$5{,}0\cdot10^{-3}$	2,9	8,0	–	–	150
10	$1{,}5\cdot10^{-2}$	2,9	8,4	–	–	60
11	$3{,}0\cdot10^{-2}$	2,5	8,6	–	–	10
12	$9{,}4\cdot10^{-2}$	2,5	8,8	–	–	0,94
13	0,145	2,5	9,0	–	5,0	0
14	0,27	2,5	9,3	–	6,6	0
15	0,26	2,5	9,2	–	11	0
16	0,40	2,5	9,7	–	12	0
17	0,46	2,5	9,8	–	66	0
18	0,74	2,5	10,7	–	56	0
19	3,5	2,5	13,3	–	190	0

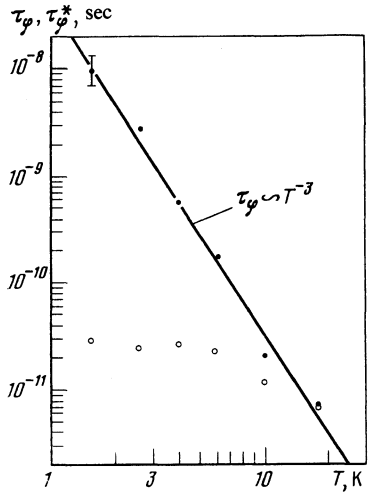

FIG. 5. Temperature dependence of the times τ_φ (●) and τ_φ^* (○) for sample No. 2.

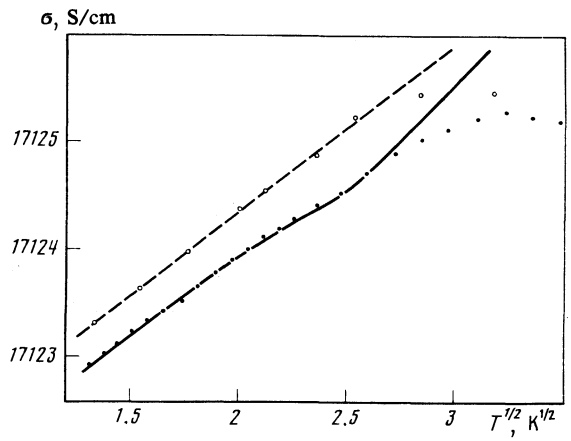

FIG. 6. Temperature dependence of the conductivity σ of sample No. 2 at $H = 0$ (●) and $H = 30$ kOe (○) ($H \gg \hbar c/4eD\tau_\varphi^*$ (10 K). The solid and dashed lines are the theoretical curves calculated according to (4) with $F = 0$ and with the values of τ_φ and τ_φ^* determined from the magnetoresistance.

The good agreement of the experimental data with expression (2) allows us to conclude that at distances greater than $L_\varphi(T,H)$ a film with $\rho < 1\cdot10^{-3}$ Ω·cm can be considered homogeneous and that $L_\varphi, L_\varphi^* > \xi$ (or $L_\varphi > b$, since far from the metal-insulator transition one has $\xi \sim b$). In fact, the values of L_φ and L_φ^* found in the magnetoresistance experiments for these films at $T \lesssim 20$ K and $H \lesssim 30$ kOe exceed the estimated dimensions of the inhomogeneity (granules).[2)] Consequently, for determining the characteristic times τ_φ and τ_φ^* from the known values of L_φ and L_φ^* one can use the diffusion coefficient D, related to the measured value ρ by $\rho D = mv_F^2/3\mathrm{Ne}^2 \approx 5.5\cdot10^{-4}$ $\Omega\cdot\mathrm{cm}^2$/sec (m is the electron mass and v_F is the Fermi velocity).[32]

The curves for $\tau_\varphi(T)$ and $\tau_\varphi^*(T)$ for sample No. 2 are shown in Fig. 5. The data on $\tau_\varphi(T)$ and $\tau_\varphi^*(T)$ enable one to obtain the temperature dependence of τ_ε and the values of τ_s and τ_{so} by a simple procedure described in Ref. 29. For the samples with $\gamma = 140$ Å we have $\tau_{so} \approx 3\cdot10^{-11}$ sec (see Table I) practically independent of ρ; these values are close to the values of τ_{so} obtained for the clean two-dimensional copper films with $a \approx 100$ Å.[29,31] This circumstance evidently stems from the fact that spin flips due to the spin-orbit interaction occur mainly in scattering by the granule boundaries, while the granule dimension b, unlike ρ and D, depends only weakly on the oxygen concentration. The spin-flip probability in scattering of this sort is $W = b/v_F\tau_{so} \sim 3\cdot10^{-4}$ for the films with $\gamma = 140$ Å ($b \approx 100$ Å), whereas an estimate of W by the formula $W \approx (\alpha Z)^4$ gives $2\cdot10^{-3}$ ($\alpha = e^2/\hbar c$, Z is the nuclear charge of the constituent atoms of the film).[33] The dependence of τ_{so} on the granule dimension can be mapped out by varying the thickness of the layers making up the film: in comparison with the values of τ_{so} for the samples with $\gamma = 140$ Å, the values of τ_{so} for $\gamma = 50$ Å are smaller by a factor of two, while for $\gamma = 10^4$ Å (sample No. 3) they are larger by a factor of 1.5. (The electron microscope data show that when γ is increased above 300–500 Å the values of both b and τ_{so} cease to change.) The growth of τ with decreasing T in thin copper films ($a \lesssim 150$ Å) has been found[29,31] to be limited by spin-flip scattering by magnetic impurities, but in the comparatively thick films such a limitation does not appear. The reason is that the scattering on magnetic impurities occurs mainly on the surface of the films, where the ESCA data indicate the presence of paramagnetic cupric oxide. Analysis of the mechanisms leading to the observed behavior of $\tau_\varepsilon(T)$ will be given in Sec. 4.2.

Let us turn now to a discussion of the temperature dependence of the conductivity in the films with $\rho < 1\cdot10^{-3}$ Ω·cm. Typical experimental curves of $\sigma(T)$ for such films are shown in Fig. 6 for the cases $H = 0$ and $H \gg \hbar c/4eD\tau_\varphi^*$ (10 K; sample No. 2). As the films were cooled from 300 to 30 K we observed an increase in the conductivity, while in the low-temperature region $\sigma(T)$ fell off something like a square-root curve. For comparing expression (4) with experiment the only adjustable parameter is the value of F, since the characteristic times τ_φ and τ_φ^* were found from an analysis of the magnetoresistance. The screening parameter F remains the only adjustable parameter in the case when the temperature dependence of σ is studied in a rather strong magnetic field. As in the case of two-dimensional copper films,[29–31] good agreement with theory is achieved for $F = 0$. The main contribution to the temperature dependence of σ is from the electron-electron interaction in the diffusion channel, since the relation $\tau_\varphi, \tau_\varphi^* \gg \hbar/kT$ holds over the entire investigated region $T = (1.5\text{–}30)$ K (see Fig. 5). The share due to the localized contribution does not exceed 10% of $\Delta\sigma(T)$ at $T \lesssim 10$ K.

4.2. $\rho \approx (1\cdot10^{-3}$ –0.5) Ω·cm

The satisfactory agreement of the experimental data with the results of the theory developed for homogeneous conductors indicates that $L_\varphi, L_T \gtrsim \xi$ at $T \gtrsim 1.5$ K and $H \lesssim 30$ kOe for samples with $\rho < 1\cdot10^{-3}$ Ω·cm. The behavior of the $\sigma(T)$ and $\sigma(H)$ curves for samples with $\rho \gtrsim 1\cdot10^{-3}$ Ω·cm does not find explanation in terms of the theory of weak localization and electron-electron interaction in macroscopically inhomogeneous metals. For example, the temperature dependence of the conductivity of samples No. 8–12 at $T \lesssim 30$ K can be approximated as $\sigma(T) = \sigma_0 + AT^{1/3}$, as is done, e.g.,

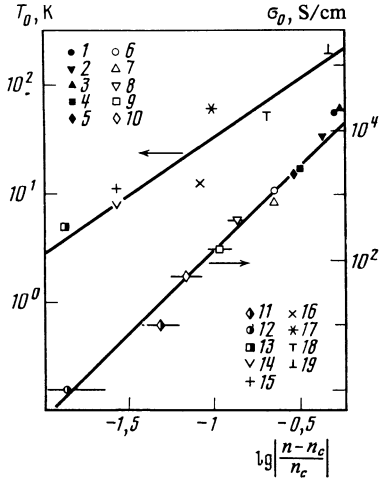

FIG. 7. Dependence of σ_0 and T_0 on the oxygen concentration $n(n_c = 12\%)$. The scatter in $\log|1 - n/n_c|$ corresponds to an accuracy of ~ 0.1 at.% in the determination of the oxygen concentration. (Each of the symbols used in this and the following figures corresponds to a particular sample, numbered as in Table I).

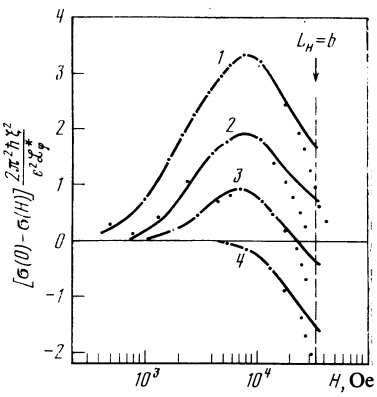

FIG. 8. Curves of $\Delta\sigma(H)$ measured at various temperatures for sample No. 10. The solid lines correspond to the theoretical curves (15) calculated for the following values of $\tau_\varphi/\tau_\varphi^*$: 1) $T = 1.8$ K, $\tau_\varphi/\tau_\varphi^* = 70$; 2) $T = 3.0$ K, $\tau_\varphi/\tau_\varphi^* = 25$; 3) $T = 6.5$ K, $\tau_\varphi/\tau_\varphi^* = 10$; 4) $T = 10$ K, $\tau_\varphi/\tau_\varphi^* = 2$.

in Refs. 14 and 34. However, because comparison with the theory yields values of σ_0 much larger than the temperature dependent term $AT^{1/3}$, one cannot assume that such a dependence is due to the critical behavior of σ near a metal-insulator transition of the Anderson type in a homogeneous system. In view of the granular structure of the films in question, it is natural to assume that the observed behavior of the conductivity is due to quantum effects in the presence of macroscopic inhomogeneities of the sample and that the metal-insulator transition is due to the vanishing of the infinite cluster of granules connected together by metallic bridges.

Figure 7 shows a plot of $\sigma_0(n - n_c)$ obtained by extrapolation to $T = 0$ of the corresponding $\sigma(T)$ curves (n is the oxygen concentration in the film). The experimental data are satisfactorily described by a function of the form $\sigma_0 \sim (1 - n/n_c)^t$, where $t \approx 2.3 \pm 0.3$. This value of the critical exponent of the conductivity is consistent with the value $t \approx 1.9$ obtained[2,35] from percolation theory and also with the experimentally determined[36] value t 1.9 ± 0.2 for cermet films fabricated by the joint sputtering of a metal and an insulator, but it differs substantially from the values $t \lesssim 1$ which are characteristic for the metal-insulator transition in macroscopically inhomogeneous conductors.[7-11] The critical concentration of the insulator Cu_2O is 0.35 ± 0.05, corresponding to a percolation threshold of 0.65 ± 0.05, which is higher than both the value for cermet films (~ 0.4–0.5)[28,36] and the theoretical value ~ 0.17.[2] Such a large value of the critical concentration of the metal in films consisting of oxidized granules was also noted in Refs. 15 and 28 and is due to the specific structural features of these films (the insulator coats the metallic granules and "disconnects" them from the infinite cluster).

For samples with $\rho \gtrsim 1 \cdot 10^{-3}$ Ω·cm the absolute values of $\Delta\sigma(H)$ and the shape of the $\sigma(H)$ curves are no longer described by expression (2). The experimental $\sigma(H)$ curves obtained at various temperatures for sample No. 10 are shown in Fig. 8. The solid lines in Fig. 8 show the functions (15) obtained with allowance for the macroscopic inhomogeneity of the samples; the dashed line is the upper limit of applicability of the theory—$L_H \approx b \approx 100$ Å. (The lower applicability limit, which is determined by the condition $\mathscr{L}_\varphi \approx L_H \gtrsim \xi$, corresponds to a value $H \approx 650$ Oe for sample No. 10 and shifts to lower values of H with increasing ρ.) Comparison of the experimental data with expression (15), which contains three unknown parameters, viz. ξ, $\mathscr{L}_\varphi$, and $\mathscr{L}_\varphi^*$, is facilitated by the fact that the maxima of the theoretical curves constructed for $\tau_\varphi/\tau_\varphi^* \gtrsim 3$ correspond to the same value of the quantity $\mathscr{L}_\varphi^{*2}/L_H^2 \approx 1.2$ (see Fig. 1). The maxima of the experimental $\sigma(H)$ curves obtained for $T \lesssim 6$ K also lie on a single vertical line, since for $T \lesssim 6$ K the time τ_φ^* and, thus, $\mathscr{L}_\varphi^* \sim (\tau_\varphi^*)^{1/(2+\tilde{t}-\tilde{\beta})}$ become practically independent of T ($\tau_{so} \ll \tau_\varphi$). Knowing the value of H which corresponds to the maxima of the low-temperature $\sigma(H)$ curves, one can determine $\mathscr{L}_\varphi^*$ for $T \lesssim 6$ K and then make further comparisons with the theory with the aid of two adjustable parameters. One of these parameters is the quantity $\mathscr{L}_\varphi^*/\xi^2$, which is the same for all the experimental $\sigma(H)$ curves obtained at $T \lesssim 6$ K. (We note that for $T \gtrsim 6$ K the temperature dependence of this quantity should also be weak—proportional to $(\tau_\varphi^*)^{1/(2+\tilde{t}-\tilde{\beta})}$—as is confirmed by experiment.) The second parameter is the ratio $\tau_\varphi/\tau_\varphi^*$. Thus in spite of the apparent indeterminacy in finding the three unknowns—two temperature-dependent ($\mathscr{L}_\varphi$ and $\mathscr{L}_\varphi^*$) and one temperature-independent (ξ)—there is a relatively simple procedure for uniquely separating them in measurements of the $\sigma(H)$ curves over a rather wide temperature interval including the temperature region in which $\mathscr{L}_\varphi^* \ll \mathscr{L}_\varphi$ ($\tau_{so} \ll \tau_\varphi$).

The values of ξ (denoted ξ_H) obtained by processing the magnetoresistance data are shown in Fig. 9. The values of ξ_H are in satisfactory agreement with the values of ξ calculated with the formula $\xi = 50(1 - n/n_c)^{-0.9}$ Å. This fact once again confirms the correctness of the assumptions we have made about the structure of the films and the percolational nature of the observed metal-insulator transition).

In principle, the experimental determination of $\mathscr{L}_\varphi$ and $\mathscr{L}_\varphi^*$ should make it possible to find the times τ_φ and τ_φ^* for a suitable choic of diffusion coefficient D. To estimate D

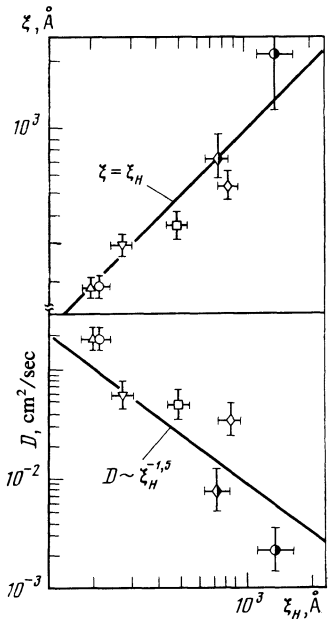

FIG. 9. Plots of $\xi = 50(1 - n/n_c)^{-0.9}$ Å and D vs ξ_H. The error in determining ξ corresponds to an uncertainty in n of 0.1%.

in the resistivity interval $\rho = (1\cdot10^{-3}$–$0.5)\ \Omega$·cm we have made use of the circumstance that for ρ between $5\cdot10^{-5}$ and $1\cdot10^{-3}\ \Omega$·cm the values of τ_{so} determined from the magnetoresistance data are practically independent of ρ (see Table I) and are close to the values of τ_{so} obtained for clean copper films with $a \approx 100$ Å.[29] As we have mentioned, this explains why the granule dimension is the same in films with different oxygen concentrations. Having assumed that τ_{so} remains nearly unchanged at about $3\cdot10^{-11}$ sec as ρ is increased further up to $0.5\ \Omega$·cm, one can obtain an estimate of D from the relation $\mathscr{L}_\varphi^* = (3/4D\tau_{so}\xi^{\bar{t}-\bar{\beta}})^{1/(2+\bar{t}-\bar{\beta})}$, which is valid for $T \lesssim 2$ K ($\tau_{so} \ll \tau_\varphi$). The values of D thus obtained are plotted against σ_H in Fig. 9. The experimental data are consistent with the dependence $D \sim \xi^{-\bar{t}+\bar{\beta}} \sim \xi^{-1.5}$ implied by percolation theory.

Knowing D, one can determine the times τ_φ and τ_φ^* in films with $\rho \approx (1\cdot10^{-3}$–$0.5)\ \Omega$·cm and analyze the resulting $\tau_\varphi(T)$ curves. The $\tau_\varphi(T)$ curves for samples No. 2, 10, and 12 are shown in Fig. 10. The very fact that τ_φ is temperature dependent indicates that the main process in the relaxation of the phase of the electron wavefunction is inelastic scattering, since the time τ_s should not depend on temperature [see formula (3)]. For the investigated films in the temperature region $T = (1.5$–$10)$ K the wavelength λ_T of a thermal phonon becomes comparable with the electron mean free path $l \sim b$ inside the granules. Unfortunately, there have been no satisfactory calculations of the inelastic electron-phonon scattering time τ_ε^{ph} in the "dirty" case ($\lambda_T > l$). The expression for τ_ε^{ph} in the "clean" case ($\lambda_T \ll l$)[37]

$$\tau_\varepsilon^{ph} = \frac{1}{6\pi\zeta(3)\lambda}\frac{\hbar\Theta_D^2}{kT^3} \qquad (16)$$

[where Θ_D(Cu) = 315 K is the Debye temperature, $\zeta(3) \approx 1.202$, and λ (Cu) ≈ 0.15 is the electron-phonon interaction constant] satisfactorily describes the power-law behavior $\tau_\varphi(T) \sim T^{-3}$ observed in films with $\rho \lesssim 1\cdot10^{-4}\ \Omega$·cm. The

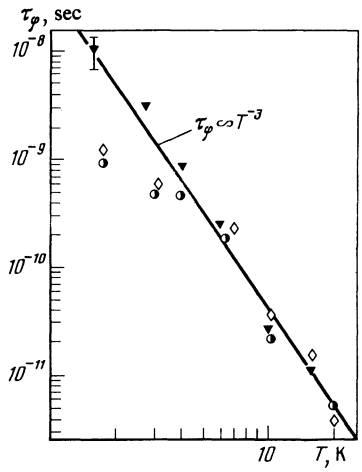

FIG. 10. Temperature dependence of τ_φ for samples No. 2, 10, and 12.

absolute values of τ_φ, however, turn out to be an order of magnitude smaller than those calculated according to formula (16).

For highly disordered films the temperature dependence of τ_φ in the low-temperature region becomes weaker, and the absolute values of τ_φ are practically independent of the resistivity over the range from $1\cdot10^{-3}$ to $0.5\ \Omega$·cm. This is apparently because in this temperature region the value of τ_φ for the films in question is determined by electron—electron collisions in a macroscopically inhomogeneous three-dimensional system.

For films with $\rho \approx (1\cdot10^{-3}$–$0.5)\ \Omega$·cm the $\sigma(T)$ curve in the interval $T \approx (1.5$–$30)$ K is described satisfactorily by the expression $\sigma = \sigma_0 + AT^\alpha$, where $\alpha \approx 1/3$ and the coefficient A turns out to be independent of σ_0 (see Fig. 11). Similar behavior has been observed for films with values of ρ in this range in all the studies[13–17,34] that have been done on the metal—insulator transition in disordered metal films. (In

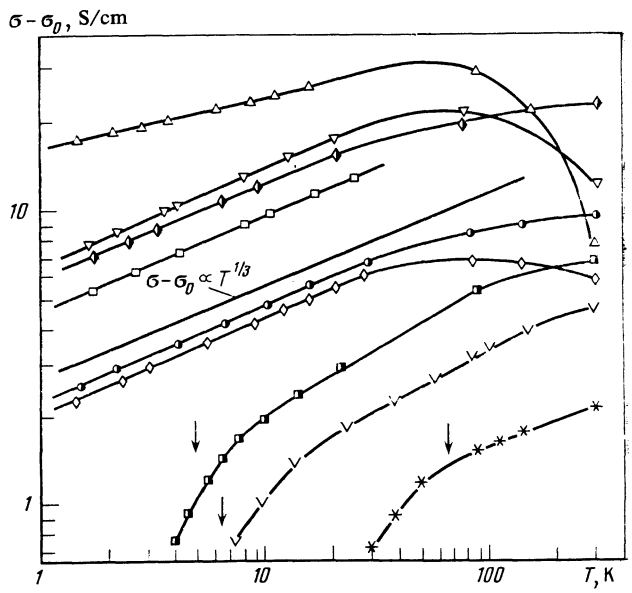

FIG. 11. Curves of $\Delta\sigma(T)$ for samples No. 7–14 and 17. The arrows correspond to $T = T_0$ for samples No. 13, 14, and 17.

Refs. 13, 15, and 17 the $\Delta\sigma(T)$ curves were approximated by a logarithmic function, which in the investigated temperature intervals differs only slightly from a power-law dependence with exponent $\alpha \approx 1/3$.) In a strong magnetic field, which suppresses the temperature dependence of the localization contribution, the exponent α changes from $\sim 1/3$ to $\sim 1/4$. It is important to note that the calculated temperature dependence of σ due to quantum effects under percolation conditions does not agree with the observed $\sigma(T)$ curve. First of all, the temperature dependence of σ turns out to be different. Second, and this is particularly important, the experiment yields values of A which do not depend on σ_0, whereas according to (10) the coefficient A should be proportional to σ_0. Further, the quantum corrections turn out to be much smaller than the experimentally observed quantity $\Delta\sigma(T)$. Allowance for interaction effects does not alter the picture described above. Thus the behavior of $\sigma(T)$ observed near the percolational metal-insulator transition apparently cannot be explained by the theory of quantum corrections to the conductivity.

4.3. $\rho \gtrsim 0.5\ \Omega\cdot$cm

For samples with $\rho \gtrsim 0.5\ \Omega\cdot$cm the conductivity observed at low temperatures (see Fig. 3) is activational in nature, with a temperature dependence $\rho(T)$ of the form

$$\rho = \rho_0 \exp(T_0/T)^{1/2}. \tag{17}$$

Analogous behavior of $\rho(T)$ has been observed on the insulator side of the transition in both semiconductors[10,11] and disordered metals.[13,15,17] Such a behavior of $\rho(T)$ follows from a treatment of the hopping conductivity with a variable hopping length in homogeneous conductors with a Coulomb gap in the electron spectrum.[2] Here $T_0 \sim e^2/\varkappa\xi$, where $\varkappa$ is the dielectric constant. Since $\varkappa \sim (n/n_c - 1)^{-\eta}$ (where η is the critical exponent of the dielectric constant) in the critical region, we have $T_0 \sim (n/n_c - 1)^{\eta+\nu}$. The applicability of this model to granular conductors was discussed in Ref. 38, and in Ref. 39 it was shown that for materials of this kind one should replace ξ in the expression for T_0 by $\xi\delta/s$, where δ is the damping length of the electron wavefunction in the insulator and s is the distance between granules. For our samples the experimental values of T_0 are given in Table I, and the dependence of T_0 on the oxygen concentration in the films is shown in Fig. 7. The increase in T_0 for the more disordered films is due to a decrease in the correlation length ξ and dielectric constant $\varkappa$ upon advancing into the dielectric region. The critical exponent of T_0 for our films was 1.2 ± 0.3, which is close to the value of $\eta + \nu$ obtained in percolation theory [$\nu = 0.8$–0.9 (Ref. 2), $\eta = 0.73 \pm 0.07$ (Ref. 40)]. The value obtained for T_0 in (17) in each case practically coincides with the upper boundary of the temperature interval in which (17) holds (see Fig. 11). For $T > T_0$, $\Delta\sigma(T)$ exhibits a power-law behavior with an exponent α close to 1/3, as in the case $\rho = (1\cdot10^{-3}$–$0.5)\ \Omega\cdot$cm.

A dependence of the form (17) has also been obtained for granular materials in a treatment of the tunneling of thermally excited charge carriers between adjacent granules with allowance for the Coulomb interaction.[41,42] This result, however, was obtained under certain assumptions about the structure of the granular metal: 1) $b/s = \text{const}$, with wide variations in the value of b,[41] or 2) b is small ($\lesssim 30$ Å),[42] which was not the case in our experiment.[3)]

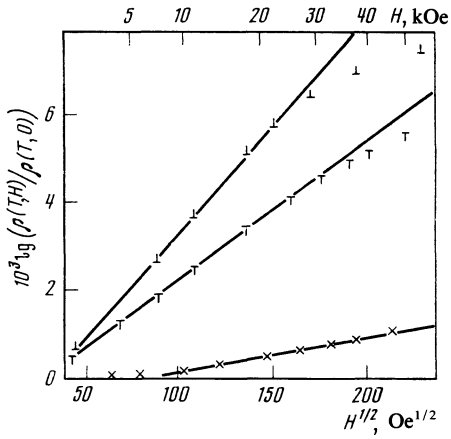

FIG. 12. Curves of $\log[\rho(T,H)/\rho(T,0)]$ vs H for samples No. 16, 18, and 19.

The magnetoresistance observed in the strong-localization region is negative at arbitrary values of H, and the curves of $\lg[\rho(T,H)/\rho(T,0)]$ versus H are similar in shape to a square-root function (Fig. 12). In the strong-localization region the appearance of magnetoresistance in classically weak magnetic fields is attributed to a possible lowering of the mobility threshold, leading to a negative magnetoresistance.[43] In the case when the temperature dependence of ρ is described by expression (17), we have for a negative magnetoresistance[43]

$$\lg[\rho(T,H)/\rho(T,0)] = -B\nu\left(\frac{eH}{\hbar c}N^{-2/3}\right)^{1/2\nu}\lg\frac{\rho(T)}{\rho_0}, \quad B = O(1), \tag{18}$$

where N is the electron concentration. The experimental values of $\log[\rho(T,H)/\rho(T,0)]$ at fixed H turn out, in agreement with (18), to be proportional to $\log[\rho(T)/\rho_0]$. For samples No. 16, 18, and 19, whose the magnetoresistance curves are shown in Fig. 12, the ratios

$$\lg[\rho(T,H)/\rho(T,0)]/H^{1/2}\lg[\rho(T)/\rho_0]$$

are practically the same, amounting to $\sim 1\cdot10^{-5}$. By assigning a value $N(\text{Cu}) = 8.5\cdot10^{22}\ \text{cm}^{-3}$ (Ref. 32), one can determine the coefficient B in formula (18); in our case we get $B \approx 0.11$.

5. CONCLUSION

We have found that the disordered $Cu_{1-x}O_x$ ($x = 0.02$–0.2) films studied in our experiments exhibit a combination of both quantum effects (electron localization and enhancement of the electron-electron interaction) and classical percolation effects. Behavior of this sort is due to the presence of both small-scale and large-scale structural inhomogeneities in these films. Here the transition from metallic to activational conductivity is classical in nature and is satisfactorily described by percolation theory. Such a metal-insulator transition is apparently characteristic of a large number of granular systems.[12–17] Far from the metal-insulator transition the observed behavior of $\sigma(T)$ and $\sigma(H)$ is described well by the theory of quantum corrections to the

conductivity as developed for the homogeneous case. As the transition is approached the condition $\xi < L$, L_T breaks down; this circumstance is responsible for the particulars of the manifestation of quantum effects in films with $\rho \approx (1 \cdot 10^{-3}$–$0.5)\ \Omega \cdot$cm. The theory developed for the manifestation of quantum effects in percolation systems gives an adequate description of the magnetoresistance of such films and enables one to determine the correlation length in them. At the same time the temperature dependence in films with $\rho \gtrsim 1 \cdot 10^{-3}\ \Omega \cdot$cm is not explained by the theory of quantum effects; this apparently indicates that the observed behavior of $\sigma(T)$ is of a different origin.

We are deeply grateful to B. I. Shklovskiĭ for a detailed discussion of the results. We are also indebted to V. N. Gubankov for interest in this study and to B. L. Al'tshuler, D. E. Khmel'nitskiĭ, and Yu. V. Sharvin for a helpful discussion.

[1)]We are indebted to V. G. Krigel' and D. V. Klyachko for the Auger-spectroscopy and ESCA studies of the films.

[2)]In fields $H \gtrsim 30$ kOe one observes deviations from (2) due to the breakdown of condition $L_H > b$.

[3)]We are indebted to B. I. Shklovskiĭ for calling our attention to this circumstance.

[1]N. F. Mott and E. A. Davis, Electronic Processes in Non-crystalline Materials, Clarendon Press, Oxford (1971) [Russian translation Mir, Moscow (1982)].
[2]B. I. Shklovskiĭ and A. L. Éfros, Elektronnye Svoistva Legirovannykh Poluprovodnikov, Nauka, Moscow (1979) [Electronic Properties of Doped Semiconductors, Springer-Verlag, New York (1984)].
[3]E. Abrahams, P. W. Anderson, D. C. Licciardello, and T. V. Ramakrishnan, Phys. Rev. Lett. **42**, 673 (1979).
[4]B. L. Al'tshuler and A. G. Aronov, Zh. Eksp. Teor. Fiz. **77**, 2028 (1979) [Sov. Phys. JETP **50**, 968 (1979)].
[5]D. E. Khmel'nitskiĭ, Pis'ma Zh. Eksp. Teor. Fiz. **32**, 248 (1980) [JETP Lett. **32**, 229 (1980)].
[6]Y. Gefen, D. J. Thouless, and Y. Imry, Phys. Rev. B **28**, 6677 (1983).
[7]T. F. Rosenbaum, R. F. Milligan, M. A. Paalanen, G. A. Thomas, R. N. Bhatt, and W. Lin, Phys. Rev. B **27**, 7509 (1983).
[8]G. A. Thomas, M. A. Paalanen, and T. F. Rosenbaum, Phys. Rev. B **27**, 3897 (1983).
[9]M. A. Paalanen, T. F. Rosenbaum, G. A. Thomas, and R. N. Bhatt, Phys. Rev. Lett. **51**, 1896 (1983).
[10]A. G. Zabrodskiĭ and K. N. Zinov'eva, Pis'ma Zh. Eksp. Teor. Fiz. **37**, 369 (1983) [JETP Lett. **37**, 436 (1983)].
[11]A. N. Ionov, I. S. Shlimak, and M. N. Matveev, Solid State Commun. **47**, 763 (1983).
[12]R. C. Dynes and J. P. Garno, Phys. Rev. Lett. **46**, 137 (1981).
[13]T. Chui, G. Deutscher, P. Lindenfeld, and W. L. McLean, Phys. Rev. B **23**, 6172 (1981).
[14]B. W. Dodson, W. L. McMillan, J. M. Moshel, and R. C. Dynes, Phys. Rev. Lett. **46**, 46 (1981).
[15]N. Savvides, S. P. McAlister, C. M. Hurd, and I. Shiozaki, Solid State Commun. **42**, 143 (1982).
[16]G. Hertel, D. J. Bishop, E. C. Spenser, J. M. Rowell, and R. C. Dynes, Phys. Rev. Lett. **50**, 743 (1983).
[17]S. L. Weng, S. Moehlecke, N. Strongin, and A. Zangwill, Phys. Rev. Lett. **50**, 1795 (1983).
[18]B. L. Al'tshuler and A. G. Aronov, Solid State Commun. **46**, 429 (1983).
[19]B. L. Al'tshuler and A. G. Aronov, Pis'ma Zh. Eksp. Teor. Fiz. **37**, 349 (1983) [JETP Lett. **37**, 410 (1983)].
[20]T. A. Polyanskaya and I. I. Saĭdashev, Zh. Eksp. Teor. Fiz. **84**, 997 (1983) [Sov. Phys. JETP **57**, 578 (1983)].
[21]T. F. Rosenbaum, R. F. Milligan, G. A. Thomas, P. A. Let, T. V. Ramakrishnan, R. N. Bhatt, K. DeConde, H. Hess, and T. Perry, Phys. Rev. Lett. **47**, 1758 (1981).
[22]S. Morita, Y. Isawa, S. Ishida, Y. Koike, Y. Takeuti, N. Mikoshiba, Phys. Rev. B **25**, 5570 (1982).
[23]G. A. Thomas, A. Kawabata, Y. Ootuka, S. Katsumoto, S. Kobayashi, and W. Sasaki, Phys. Rev. B **26**, 2113 (1982).
[24]I. L. Bronevoĭ, Zh. Eksp. Teor. Fiz. **83**, 338 (1982) [Sov. Phys. JETP **56**, 185 (1982)].
[25]B. L. Al'tshuler, A. G. Aronov, A. I. Larkin, and D. E. Khmel'nitskiĭ, Zh. Eksp. Teor. Fiz. **81**, 768 (1981) [Sov. Phys. JETP **54**, 411 (1981)].
[26]A. Kawabata, Solid State Commun. **34**, 431 (1980).
[27]S. Hikami, A. I. Larkin, and Y. Nagaoka, Prog. Theor. Phys. **63**, 707 (1980).
[28]B. Abeles, Applied Solid State Science, Vol. 6 (ed. by R. Wolfe), Academic Press, New York (1976), p. 1.
[29]M. E. Gershenzon, V. N. Gubankov, and Y. E. Zhuravlev, Zh. Eksp. Teor. Fiz. **83**, 2348 (1982) [Sov. Phys. JETP **56**, 1362 (1982)].
[30]G. Bergmann, Z. Phys. B **48**, 5 (1982).
[31]D. Abraham and R. Rosenbaum, Phys. Rev. B **27**, 1413 (1983).
[32]N. W. Ashcroft and N. D. Mermin, Solid State Physics, Holt, Reinhart, and Winston, New York (1976) [Russian translation Mir, Moscow (1979)].
[33]A. A. Abrikosov and L. P. Gor'kov, Zh. Eksp. Teor. Fiz. **42**, 1088 (1962) [Sov. Phys. JETP **15**, 752 (1962)].
[34]Y. Imry and Z. Ovadyahu, J. Phys. C **15**, L327 (1982).
[35]M. Sahimi, B. Hughes, L. E. Scriven, and H. T. Davis, J. Phys. C **16**, L521 (1983).
[36]B. Abeles, H. L. Pinch, and J. I. Gittleman, Phys. Rev. Lett. **35**, 247 (1975).
[37]C. J. Pethick and H. Smith, Ann. Phys. (N.Y.) **119**, 133 (1979).
[38]O. Entin-Wohlman, Y. Gefen, and Y. Shapira, J. Phys. C **16**, 1161 (1983).
[39]B. I. Shklovskiĭ, Fiz. Tverd. Tela (Leningrad) **26**, 585 (1984) [Sov. Phys. Solid State **26**, 353 (1984)].
[40]D. M. Grannan, J. C. Garland, and D. B. Tanner, Phys Rev. Lett. **46**, 375 (1981).
[41]P. Sheng, B. Abeles, and Y. Arie, Phys. Rev. Lett. **31**, 44 (1973).
[42]E. Simanek, Solid State Commun. **40**, 1021 (1981).
[43]B. L. Al'tshuler, A. G. Aronov, and D. E. Khmel'nitskiĭ, Pis'ma Zh. Eksp. Teor. Fiz. **36**, 157 (1982) [JETP Lett. **36**, 195 (1982)].

Translated by Steve Torstveit